Mechanism of lipid induced insulin resistance: Activated PKCϵ is a key regulator

Suman Dasgupta, Sushmita Bhattacharya, Sudipta Maitra, Durba Pal, Subeer S. Majumdar, Asis Datta, Samir Bhattacharya

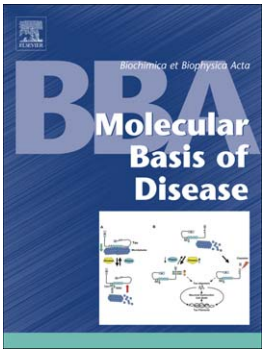

Mechanism of lipid induced insulin resistance: Activated PKCϵ is a key regulator

Suman Dasgupta, Sushmita Bhattacharya, Sudipta Maitra, Durba Pal, Subeer S. Majumdar, Asis Datta, Samir Bhattacharya

PII: S0925-4439(11)00002-0
DOI: doi: 10.1016/j.bbadis.2011.01.001
Reference: BBADIS 63226

To appear in: *BBA - Molecular Basis of Disease*

Received date: 16 November 2010
Revised date: 21 December 2010
Accepted date: 3 January 2011

Please cite this article as: Suman Dasgupta, Sushmita Bhattacharya, Sudipta Maitra, Durba Pal, Subeer S. Majumdar, Asis Datta, Samir Bhattacharya, Mechanism of lipid induced insulin resistance: Activated PKCϵ is a key regulator, *BBA - Molecular Basis of Disease* (2011), doi: 10.1016/j.bbadis.2011.01.001

Mechanism of lipid induced insulin resistance: Activated PKCε is a key regulator

Suman Dasgupta [a], Sushmita Bhattacharya [a], Sudipta Maitra [a], Durba Pal [a], Subeer S. Majumdar [c], Asis Datta [d,*], Samir Bhattacharya [a,b,*]

[a] *Cellular and Molecular Endocrinology Laboratory, Department of Zoology, School of Life Science, Visva-Bharati University, Santiniketan - 731235, India;*

[b] *North-East Institute of Science and Technology, Jorhat- 785006, India;*

[c] *Division of Cellular Endocrinology, National Institute of Immunology, Aruna Asaf Ali Marg, New Delhi - 110067, India;*

[d] *National Institute of Plant Genome Research, Aruna Asaf Ali Marg, New Delhi - 110067, India;*

***Address for joint corresponding authors**:

Professor Samir Bhattacharya, Visva-Bharati University, Santiniketan - 731235.

Phone: +91-3463-261268; Fax: +91-3463-261176;

E-mail: bhattacharyasa@gmail.com and

Professor Asis Datta, National Institute of Plant Genome Research, Aruna Asaf Ali Marg, New Delhi - 110067. Phone: +91-11-26742267; Fax: + 91-11-26741759;

E-mail: asis_datta@rediffmail.com

Abstract

Fatty acids (FAs) are known to impair insulin signaling in target cells. Accumulating evidences suggest that one of the major sites of FAs adverse effect is insulin receptor (IR). However, the underlying mechanism is yet unclear. An important clue was indicated in leptin receptor deficient (*db/db*) diabetic mice where increased circulatory FAs was coincided with phosphorylated PKCε and reduced IR expression. We report here that central to this mechanism is the phosphorylation of PKCε by FAs. Kinase dead mutant of PKCε did not augment FA induced IRβ downregulation indicating phosphorylation of PKCε is crucial for FA induced IRβ reduction. Investigation with insulin target cells showed that kinase independent phosphorylation of PKCε by FA occurred through palmitoylation. Mutation at cysteine 276 and 474 residues in PKCε suppressed this process indicating participation of these two residues in palmitoylation. Phosphorylation of PKCε endowed it the ability to migrate to the nuclear region of insulin target cells. It was intriguing to search about how translocation of phosphorylated PKCε occurred without having canonical nuclear localization signal (NLS). We found that F-actin recognized phospho-form of PKCε and chaperoned it to the nuclear region where it interact with HMGA1 and Sp1, the transcription regulator of IR and HMGA1 gene respectively and impaired HMGA1 function. This resulted attenuation of HMGA1 driven IR transcription that compromised insulin signaling and sensitivity.

Key words**:** Fatty acid; HMGA1; Insulin resistance; IRβ; PKCε.

1. Introduction

Interaction of insulin with its receptor tyrosine kinase triggers intracellular cascade of kinases that leads to cellular uptake of glucose in insulin target cells. Several authors have demonstrated that downregulation of IR is accompanied by diminished insulin signaling causing insulin resistance (1-4). A few significant information relevant to this are enumerated below (a) IR knockout in mice liver leads to the development of insulin resistance and type 2 diabetes (3), (b) induction of endoplasmic reticulum stress abrogates IR expression that causes insulin resistance (5), (c) number of IR per adipocyte significantly decreases in the obese patients (1), (d) this has been further confirmed with fibroblasts, the precursor cells of adipocytes, collected from insulin resistant patients showed both quantitative and qualitative defects of IR (6), (e) defects in IR gene expression have been detected in insulin resistant patients (7). (f) HMGA1, architectural transcription factor of IR gene, has been found to be deficient in diabetic patients and this effected reduced IR expression (8). Hence, from all these reports it appears that reduction of IR is associated with insulin signaling defect which produces insulin resistance and diabetic in human being.

To search the cause for such reduction, many suggested lipid as the major player. Reduced IR expression has been observed in mice with abdominal obesity and hepatic steatosis (9). Saturated long chain FAs are shown to be associated with the defects of insulin signaling. Palmitate decreased IR protein and mRNA expression in hepatocyte and skeletal muscle cell lines that attenuates insulin signaling (4,10) and a concentration dependent decline of IR occurs in insulin target cells due to palmitate (11). Lipid transfection to skeletal muscle cells and adipocytes reduces IR expression that impairs

insulin responsiveness (12). These information are consistent in implying that FA induced reduction of IR is one of the causes to develop insulin resistance but how lipid is related to IR downregulation in insulin target cells is still unclear.

A few reports indicated interplay of protein kinase Cε (PKCε) in mediating the lipids induced IR damage. It has been shown that IR expression is inversely correlated to PKCε in diabetic obese rats (13). Moreover, lipid induced hepatic insulin resistance could be prevented by knocking down of PKCε (14). PKCε is implicated in the impairment of HMGA1 that coincided with the reduced IR expression (15). These fragmented reports appear to be meaningful and there might be an association between lipid and PKCε which imposes defects in IR. Here we report that lipid induced phosphorylation of PKCε occurs due to palmitoylation. Phosphorylated PKCε is transported to the nuclear region by F-actin where it impaired HMGA1 resulting reduced IR expression that significantly decreases insulin sensitivity in target cells.

2. **Materials and methods**

2.1 Materials

All tissue culture materials were obtained from Gibco-BRL, Life Technologies Inc., Gaithersburg, USA. Anti-PKCε (anti-rabbit), anti-pPKCε (Ser-729, anti-rabbit), anti-HMGA1 (anti-rabbit), anti-pIRβ (Tyr 1150/1151, anti-mouse), anti-IRβ (anti-rabbit), anti-p-c-Jun (Ser-63/73, anti-rabbit) and anti-p-c-Fos (Thr-232, anti-rabbit) antibodies were purchased from Santa Cruz Biotechnology Inc., California, USA. Anti-F-actin (anti-mouse) and anti-pSp1 (Thr-453, anti-rabbit) antibodies were from Abcam Inc., Cambridge, USA. All fluorescent (goat anti-rabbit fluorescence iso-

thiocyanate (FITC); rabbit anti-mouse rhodamine) and alkaline phosphatise conjugated secondary antibodies were purchased from Sigma Chemical Co., St. Louis MO, USA. [γ-^{32}p]-ATP (Specific activity: 3800 Ci/mmol) was procured from BRIT, India. [^{3}H]-Palmitic acid (Specific activity: 52 Ci/mmol) and [^{3}H]-2-deoxyglucose (Specific activity: 12.0 Ci/mmol) were purchased from GE Healthcare Biosciences Ltd., Kowloon, Hong Kong. All fatty acids, cerulenin, triacsin C and cytochalasin B were from Sigma Chemical Co., St. Louis MO, USA. PKCε translocation inhibitor peptide EAVSLKPT (εV1) was purchased from Calbiochem, Darmstadt, Germany. All the restriction enzymes and Gaussia Luciferase assay kit were from New England Biolabs (UK) Ltd. Hertfordshire, England, UK. Serum glucose level was measured by using glucose oxidase method and serum FFA levels was measured by acyl-CoA synthase and acyl-CoA oxidase methods (Roche Diagnostics, Indianapolis,USA). The other chemicals and reagents used were purchased from Sigma Chemical Co., St. Louis MO, USA.

2.2 Mice

Diabetic male *Lpr^{db}* mice (BKS.Cg-*m* +/+ *Lepr^{db}*/J, stock # 000642) and their age matched non-diabetic mice (C57BLKS/6J) obtained from Jackson's laboratory were housed in group of 5 individuals/cage under 12 h light/dark cycle at 23±2^{o}C (humidity 55±5%) with *ad libitum* access to food and water. All experiments were performed following the guidelines prescribed by the Animal Ethics Committee.

2.3 FFA treatments

FFAs were conjugated with FFA-free bovine serum albumin following the method described by Chavez *et al*, 2003 (16). Briefly, FFAs were dissolved in ethanol and diluted 1:100 in 1% FBS-DMEM containing 5% (w/v) bovine serum albumin.

2.4 Cell culture and treatments

The rat L6 skeletal muscle, human HepG2 and mouse 3T3-L1 cell lines were kind gifts from Dr. Partha P. Banerjee, Georgetown University Medical Center, Washington, DC, USA. Cells were cultured in a similar manner as described by us previously (15). Briefly, L6 skeletal muscle cells were cultured in DMEM medium supplemented with 10% fetal calf serum, 25mM glucose, 1% penicillin-streptomycin (Invitrogen) in a humidified 95% O_2/5% CO_2 atmosphere at 37°C. Cells attaining 60-70% confluence were differentiated in DMEM containing 2% fetal bovine serum and 1% pen-strep for 4-6 day prior to all experiments. HepG2 and 3T3-L1 adipocytes were cultured in a similar manner as described previously (17). Cells were incubated for 6h with 0.3mM of concentration of different fatty acids conjugated with 5% BSA with or without inhibitors mentioned at specific places. PKCε siRNA, wild type and mutated pCMV-PKCε vectors were transfected to L6 myotubes ($2x10^5$ cell/well) by using Lipofectamine 2000 (Invitrogen, Carlsbad, CA) following manufacturer's protocol. After 48 h of transfection, cells were washed with DMEM. Transfected cells were then used for different experiments. On termination of incubations, cells were washed twice with ice-cold PBS and harvested with trypsin (0.25%)–EDTA (0.5 mM). Cell pellets were resuspended in lysis buffer (1% NP-40, 20 mM HEPES (pH 7.4), 2 mM EDTA, 100 mM NaF, 10 mM sodium

pyrophosphate, 1 mM sodium orthovanadate, 1 μg/ml leupeptin, 1 μg/ml aprotinin, 1 μg/ml pepstatin and 1 mM PMSF), sonicated on ice and lysates were centrifuged for 10 min at 10,000 g and protein concentrations of supernatant were determined by the method of Lowry *et al*, 1951 (18).

2.5 Electrophoresis and immunoblotting

60 μg of protein from the lysates of control and treated cells were resolved on 10% or 12.5% SDS–PAGE and transferred to PVDF membranes (Millipore, Bedford, MA) with the help of Semi-Dry trans blot Apparatus (Bio-Rad Trans-Blot® SD-Cell). The membranes were first incubated with respective primary antibodies at 1:1000 dilutions followed by incubation with either alkaline phosphatase conjugated goat anti-rabbit or rabbit anti-mouse secondary antibodies at same dilutions using SNAP i.d.™ Apparatus (Millipore, Bedford, MA). The protein bands were detected by using 5-bromro 4-chloro 3-indolyl phosphate/nitroblue tetrazolium (BCIP/NBT).

2.6 Reverse transcription-PCR (RT-PCR) and real time quantitative PCR (qPCR)

Total RNA was extracted from different incubations using TRI Reagent (Sigma–Aldrich) according to the manufacturer's instructions. RT-PCR was performed using Revert Aid™ first strand cDNA synthesis kit (Fermentas Life Sciences, Hanover, MD). Gene expression was quantified using Real time PCR (Applied Biosystems Inc. CA). PCR was performed using gene-specific primers with the following reaction conditions: initial activation step at 95°C for 15 min, then 40 cycles of denaturation at 95°C for 30 s, annealing at 55°C for 30 s and final extension at 72°C for 30 s. *Gapdh* was

simultaneously amplified in separate reactions. The C_t value was corrected using corresponding *Gapdh* controls. Primer sequences used were as shown in Table 1.

2.7 [^{3}H] 2-deoxyglucose uptake

[^{3}H] 2-deoxyglucose (2-DOG) uptake in L6 myocytes was performed according to the previous description (19). L6 myocytes were serum starved overnight in Kreb's Ringer Phosphate (KRP) buffer (12.5mM HEPES, pH 7.4, 120mM NaCl, 6mM KCl, 1.2mM $MgSO_4$, 1 mM $CaCl_2$, 0.4 mM NaH_2PO_4, 0.6 mM Na_2HPO_4) supplemented with 0.2% bovine serum albumin. Cells were incubated in absence or presence of palmitate (0.30mM) for 4 h followed by 30 min incubation with porcine insulin (100 nM). After 25 min, [3H] 2-DOG (0.4 nmol/ml) was added to each of the incubations 5 min before the termination of experiment. Cells were washed thrice with ice-cold KRP buffer in the presence of 0.3 mM phloretin to correct the glucose uptake data from simple diffusion and non-specific trapping of radioactivity. Cells were harvested with trypsin (0.25%)–EDTA (0.5 mM), solubilized with 1% NP-40 and 2-DOG uptake was measured in a Liquid Scintillation counter (Perkin Elmer, Tri-Carb 2800TR).

2.8 Metabolic labeling

L6 skeletal muscle cells were incubated with 0.8 mCi/ml [3H]-palmitic acid for varied time periods at 37°C and on termination of incubations cells were washed with PBS to remove the free label. PKCε was immunoprecipitated and subjected to electrophoresis followed by fluorography. We used CSS-palm palmitoylation algorithm (20) to predict the cysteine residues within the entire coding sequence of PKCε as

probable site of palmitoylation and it was set to the highest cutoff in CSS-palm algorithms.

2.9 Co-immunoprecipitation

Cells were incubated without or with palmitate or palmitate plus εV1. On termination of incubation, nuclear fractions were extracted (19) and used for immunoprecipitation. Briefly, 200μg of nuclear protein was incubated overnight at 4°C with either 2μg of anti-F-actin or anti-HMGA1 antibody. Around 50μl of Protein A Sepharose was then added to each tube and incubated at 4°C for 2h followed by centrifugation at 10,000g. Immunocomplexed F-actin or HMGA1 was resuspended in 500μl of 0.1% CHAPS in PBS and washed thoroughly in PBS. Immunoprecipitates were boiled in 5xSDS sample buffer and resolved in 10% SDS-PAGE followed by immunoblotting with either anti-PKCε or anti-pPKCε antibody.

2.10 Confocal Microscopy

Confocal microscopy was performed by following the description reported previously by us (21). Briefly, control and treated L6 skeletal muscle cells were incubated with both anti-rabbit pPKCε and anti-mouse F-actin antibodies for 2 h followed by double staining with FITC-conjugated goat anti-rabbit and Rhodamine conjugated rabbit anti-mouse antibodies for 1 h. Coverslips were then mounted on glass slides and examined under laser scanning confocal microscope (Leica Corp., Rockleigh,NJ).

2.11 Immunoaffinity Chromatography

To prepare pPKCε rich fraction, L6 skeletal muscle cells were incubated for 6 h with palmitate. On termination of incubation, cells were lysed and supernatant was isolated. The supernatant was passed through Microcon YM-50 followed by YM-100 filter devices to remove the protein below and above of 50kD and 100kD respectively. Filtrate from YM-100 was used for immunoaffinity chromatography where cyanogen bromide (CNBr) activated Sepharose 4B beads were conjugated with the anti-pPKCε antibody by following the procedure previously described by us (19). Purified pPKCε was used for Surface plasmon resonance analysis.

2.12 Surface Plasmon Resonance (BIAcore) Study

To observe the interaction between pPKCε and HMGA1, Surface plasmon resonance experiments were performed on a BIAcore™ 3000 instrument (BIAcore, Inc., Uppsala, Sweden) using NTA sensor chip following manufacturer's instructions. Briefly the NTA sensor chip was equilibrated with running buffer containing 10mM HEPES (pH-7.5), 150mM NaCl, 0.005% Surfactant P20, 50mM EDTA followed by priming the chip with 0.1M $NiCl_2$ and again equilibrated with running buffer, then pure His-HMGA1 protein flowed over the Ni^{2+} coated NTA sensor chip surface at a flow rate of 5µl/min. The final amount of His-HMGA1 protein covalently immobilized on the surface was 600RU. To observe the pattern of HMGA1-pPKCε binding, pPKCε from 50 to 400nM concentrations was run over the HMGA1 immobilized Ni^{2+} primed NTA chip at a flow

rate of 5µl/min for 10 min. Binding between these two proteins was monitored in real time via the changes in refractive index which was proportional to the changes in mass concentration at the sensor chip surface and plotted as Resonance Unit (RU) versus time. The sensorgram was corrected by subtracting the initial level of SPR signal before injection of the pPKCε. Binding kinetics was analyzed for one-to-one Langmuir binding model provided with BIA evaluation software.

2.13 Immunocomplex kinase assays

L6 skeletal muscle cells were incubated with palmitate in presence of [γ^{32}p]-ATP and on termination of incubation, cytosolic fractions were isolated and subjected to Microcon filter devices (Millipore, Bedford, MA) through YM-50 and then YM-100, filtrate from YM-100 was collected and subjected to immunoprecipitation with anti-pPKCε antibody. Immunoprecipitated ^{32}pPKCε was used for immune-complex kinase assays under the following reaction conditions in a total volume of 30µl: 10mM $MgCl_2$, 10µg HMGA1 or Sp1 and 10µCi of [γ-^{32}P]ATP (80µM) at 25°C. The kinase reaction was stopped by 1x SDS sample buffer and resolved on 10% SDS-PAGE, transferred to PVDF membrane, followed by autoradiography. Radioactive spot corresponding to HMGA1 or Sp1 was cut from the PVDF membrane and radioactivity was measured in a liquid scintillation counter.

2.14 Chromatin Immunoprecipitation (ChIP) assay

ChIP assay was performed using a ChIP assay kit (Upstate, Temecula, CA) according to the manufacturer's protocol using anti-HMGA1 antibody. The primers

(forward: 5'-AACCACCTCGAGTCACCAAAA-3' and reverse: 5'-AGAGAGAGGGAAAGCTTGCAG-3') were used to amplify the immunoprecipitated insulin receptor promoter sequence. The PCR products were resolved on ethidium bromide stained 1.5% agarose gel and image was captured by Bio-Rad Gel documentation system.

2.15 Electrophoretic mobility shift assay (EMSA)

Nuclear extracts were prepared from control, palmitate, and palmitate plus εV1 treated cells as described previously (22). EMSA was performed by using nuclear extracts prepared from different incubations using oligonucleotide probes specific for Sp1 binding

site (forward: 5'-ATTTGCATGGCCCCGCCCCCTGAGT-3', reverse: 5'-ACTCAGGGGGCGGGGCCATGCAAAT-3') within the HMGA1 promoter. The probes were end labeled with [γ^{32}P]-ATP with T4 polynucleotide kinase and incubated with 10μg of nuclear extracts in a 20μl of binding reaction for 45 min on ice. For supershift assay, 2μg of anti-Sp1 antibody was added to the nuclear extract and the reaction mixture was resolved on 5% polyacrylamide gel and visualized by Phosphorimager (GE Healthcare, USA).

2.16 Site directed mutagenesis

A pCMV6-PKCε construct containing 5537 bp of human protein kinase C, epsilon gene (Genbank/EMBL NM_005400.2) was purchased from OriGene Technologies, Inc, Rockville, MD, USA. This vector construct was used as template for

the generation of mutant plasmids with the help of QuikChange site-directed mutagenesis system (Stratagene, CA, USA). For mutated PKCε plasmid construction, sense oligos included oligohPKCεS729A (5'-GAGGAATTCAAAGGTTTCGCCTACTTTGGTGAAGACC-3'), oligohPKCεΔ729 (5'-GGAGGAATTCAAAGGTTTCTACTTTGGTGAAGACCTGA-3') oligohPKCεC13A (5'-GGCCTTCTTAAGATCAAAATCGCCGAGGCCGTGAGCT-3'), oligohPKCεC276A (5' AGGGTTTGCAGTGTAAAGTCGCCAAAATGAATGTTCACCGTC-3'), oligohPKCεC474A (5'-ACCTTACCCAACTCTACGCCTGCTTCCAGACCAAGG-3'), oligohPKCεC652A (5'-CAAGCGCCTGGGCGCTGTGGCATCGCAG-3').

2.17 Plasmid construct, Transfection and Reporter assay

IRP-GLuc plasmid was generated by following a previously described method with some modifications (23). Briefly, the insulin receptor promoter sequence was amplified by PCR taking phINSRP-1 as a template with forward (5'-GGGGGAATTCGGCCATTGCACTCCA-3') and reverse (5'-AATTGGATCCTGCGGGAGCGCGGGG-3') primers. The PCR products were digested with *Eco*RI/*Bam*HI and cloned into the pGLuc vector yielding pIRP-GLuc. The sequence of cloned promoter region was confirmed by sequencing. Cells were transfected for 72 hours with pIRP-GLuc plasmid (0.25 mg/well) using LipofectamineTM 2000 and luciferase activity was measured from the media of incubated cells.

2.18 Statistical analysis

All data were derived from at least three independent experiments and analyzed by one-way analysis of variance (ANOVA); where the F value indicated significance, means were compared by a post hoc multiple range test. All values were means ± SEM.

3. **Results**

3.1. *Correlation between fatty acid, PKCε phosphorylation and downregulation of IR*

To study lipid's association in IR degradation, we selected genetically modified leptin receptor deficient *db/db* mice which are extremely insulin resistant and obese in comparison to their control littermates (Fig.1A,B). There was a drastic reduction of IRβ protein and gene expression in insulin target tissues of *db/db* mice as compared to their control (Fig.1C). This was coincided with significant increase in circulatory FFA level, where palmitate and myristate were prevalent (Fig.1D,E). Interestingly, there was a significant amount of phosphorylated PKCε (pPKCε) in insulin target tissues of *db/db* mice as compared to their control, while its non-phospho form did not show such difference (Fig.1F). Nutritionally induced high fat diet (HFD) rats also exhibited similar trend (Fig.S1A). These results from *in vivo* mice model provided two valuable information - (i) two long chain FAs are important in producing damage and (ii) association of phospho-PKCε with IRβ reduction. These findings prompted us to examine the effect of saturated and unsaturated FAs on the reduction of IRβ in L6 myotubes. Maximum reduction occurred with two long chain saturated fatty acids, palmitate and myristate (Fig.2A). These FAs greatly increased PKCε phosphorylation with concurrent reduction of IRβ expression in insulin target cells (Fig.2B,C). This emphasizes the involvement of pPKCε with IRβ downregulation. It could be seen from

Fig 2D that an unsaturated fatty acid, oleate, also phosphorylated PKCε although with the same concentration it showed no effect on IR expression (Fig. 2A). To observe acute and chronic effects of FFA on insulin resistance, we incubated L6 myotubes with different concentrations of palmitate (0.25 to 1.0 mM) at 4h, 8h and 16h time periods in the presence of insulin. Palmitate inhibited insulin stimulated [^{3}H] 2-deoxyglucose (2-DOG) uptake in a dose dependent manner, however even lower doses of it i.e., 0.25 and 0.5mM showed greater inhibition due to chronic treatment for 16h.

It was evident that higher concentration of palmitate may cause cellular apoptosis (24,25), however, varied concentrations of palmitate conjugated with BSA demonstrated that exposure till 0.4mM had no effect on caspase 3 activity, a marker of apoptosis, in L6 myotube whereas 0.5mM showed a marginal effect (Fig.2D). We therefore selected 0.3mM concentration of palmitate conjugated BSA in our experiments as it will have no apoptotic effect during incubation periods (Fig. S1B).

3.2 IRβ degradation by FAs is executed through pPKCε

We, therefore, felt it to be necessary to study whether pPKCε is mediating palmitate effect on downregulation of IRβ expression. To investigate this, PKCε was mutated or deleted at serine 729 phosphorylation site and transfected to L6 myotubes. Incubation of these transfected cells with palmitate did not increased pPKCε or inhibited IRβ expression (Fig 3A). Forced expression of PKCε in L6 myotubes followed by palmitate incubation markedly reduced IRβ expression, even less than palmitate alone effect while in PKCε knockout (KO) cells palmitate failed to reduce IRβ expression. These results strongly indicate that population of pPKCε could be related to the

magnitude of IRβ reduction (Fig 3B). We then examined palmitate effect on downstream insulin signaling molecules and found that palmitate also inhibited insulin stimulated activation of IRS1 and Akt along with the IRβ (Fig. 3C). Taken together, palmitate induced phosphorylation of PKCε appears to be a key step in FA induced IRβ degradation which resulted impairment of downstream signaling molecules.

3.3 Lipid induced phosphorylation of PKCε is due to palmitoylation

Cellular phosphorylation of PKC is always dependent on PDK1; in contrast, FA induced phosphorylation appears to be not through PDK1 (15,26). Myristoylated PKCε has been shown to be constitutively phosphorylated in PDK1 knock out cells (26). Here we show that radiolabeled palmitate incubation of L6 myotubes effected palmitoylation of PKCε (Fig 4A). Addition of HCl, NaOH or hydroxylamine inhibited the palmitoylation indicating presence of thioester bond between radiolabeled palmitate and PKCε (Fig 4B). That palmitoylation of PKCε leads to its phosphorylation was evident from the effect of palmitoylation inhibitors, triacsin C and cerulenin, which suppressed palmitoylation and subsequently inhibited phosphorylation of PKCε (Fig. 4C, S1B). To search the possible site(s) of palmitoylation on PKCε, we mutated four probable cysteine residues in PKCε i.e., 13, 276, 474 and 652 (Fig. 4D) and transfected them to L6 myotubes followed by incubation with [^{14}C]-palmitate. Determination of palmitoylated PKCε through immunoprecipitation followed by flurography and immunoblot for pPKCε suggest that mutation at 276 and 474 cysteine residues completely abolished both palmitoylation and phosphorylation whereas mutation at 13 and 652 had no effect (Fig.

4E). Hence, 276 and 474 cysteine residues are the sites for palmitoylation which leads to PKCε phosphorylation.

3.4 pPKCε translocation to nuclear region is chaperoned by F-actin

Previously, we have observed that phosphorylation of PKCε has endowed it the ability for nuclear translocation (15) but could not understand how it occurs in the absence of canonical nuclear localization signal (NLS). From some earlier information it occurred that F-actin, which has 13 NLS, may be a transporter of pPKCε since phorbol ester induced activated PKCε remains bound to F-actin (27,28) and they could be detected as co-localized in the nuclear region (29). Coimmunoprecipitation study indicates that in palmitate and myristate incubated L6 myotubes, F-actin formed a complex with pPKCε but not with its non-phospho form (Fig 5A). This was also observed with 3T3-L1 adipocytes (Fig S1C). F-actin destabilizing agent, Cytochalasin B (cytoB) and PKCε translocation inhibitor, εV1 blocked PKCε translocation to nuclear region (Fig 5B). Confocal microscopy study exhibited weak and diffused staining of pPKCε in the cytoplasm of control cells and a total absence of it in the nuclear region, while in palmitate incubated cells a considerable amount of pPKCε was detected in the nuclear region and found to be colocalized with F-actin (Fig. 5C). These results provided an additional support to the above contention that only phospho-form of pPKCε is chaperoned to nuclear region by F-actin in palmitate incubated cells.

3.5 pPKCε entry into the nuclear region effected HMGA1 impairment

Biological relevance of pPKCε translocation to nuclear region of insulin target cells was previously indicated by demonstrating its association with HMGA1 (15). HMGA1 is a transcriptional regulator of IR gene (8,30,31). Here we show that pPKCε form a complex with HMGA1 in the nuclear extract of palmitate incubated cells which was inhibited by cytochalasin B and εV1 (Fig. 6A). To assess the binding affinity between pPKCε and HMGA1, we used surface plasmon resonance analysis (SPR, BIAcore). Pure His-HMGA1 was tethered to a Ni^{2+}-NTA sensor chip via their NH_2 terminal His_6 moieties and pPKCε was flowed over the sensor surface with various concentrations (50-400nM). The K_D value was found to be 10nM indicating a high affinity binding between pPKCε and HMGA1 (Fig. 6B). Immunoblot of palmitate incubated cells demonstrated a shift of HMGA1 protein band along with its weak expression which implied HMGA1 phosphorylation and reduction respectively (Fig 6C). Suppression of HMGA1 gene expression was also witnessed by RT-PCR and its prevention by cerulenin or triacsin C imply interplay of pPKCε. (Fig 6C). Phosphorylation of HMGA1 by pPKCε was detected by the transfer of radiolabeled phosphate in cell free incubation indicating that HMGA1 is a substrate of activated PKCε (Fig 6D). In searching the basis of reduced HMGA1 expression we found increased phosphorylation of Sp1 but not in Jun and Fos (Fig 7A) which was again indicated by the transfer of radiolabeled phosphate from ^{32}pPKCε to Sp1 (Fig 7B). Sp1 binding to HMGA1 promoter was significantly reduced in palmitate incubated cells, while it was prevented in cells pretreated with εV1. Addition of anti-Sp1 antibody supershifted the binding complex indicating that this band was constituted by Sp1 (Fig. 7C). These results suggest that the phophorylation of Sp1 by pPKCε inhibits its binding to HMGA1

promoter resulting reduction of its gene expression. There are evidences that phosphorylation of Sp1 deactivates it and decrease it's binding to DNA. Results described so far indicate that pPKCε is a key player in FA induced damage of insulin signaling.

3.6 Defects in HMGA1 due to pPKCε abrogate IRβ expression

Since F-actin-pPKCε complex has greater ability for phosphotransferase activity (27), it is expected both HMGA1 and Sp1 phosphorylation would take place more efficiently and that would produce defects in HMGA1. To examine this, we performed chromatin immunoprecipitation (ChIP) assay and observed a reduction of HMGA1 binding to IRβ promoter in palmitate treated cells. This was prevented by cerulenin, triacsin C, cytochalasin B and εV1 indicating that phosphorylation followed by nuclear translocation of pPKCε is involved in inhibiting HMGA1 binding to IRβ promoter (Fig. 8A). Transfection of pIRP-Gluc plasmid in L6 myotubes followed by IRβ reporter assay demonstrated a significant decrease in luciferase activity due to palmitate incubation. Attenuation of IRβ promoter activity could also be prevented by cerulenin, triacsin C, cytoB and εV1, suggesting once again the association of pPKCε in decreasing IRβ promoter activity (Fig. 8B). All these suggest a deleterious effect of pPKCε on IRβ expression.

3.7 pPKCε mediated IRβ downregulation impairs insulin sensitivity

To examine whether palmitate-pPKCε-HMGA1 mediated reduction of IRβ expression could reduce insulin sensitivity, we investigated GFP-Glut4 migration to cell membrane

and [^{3}H]-2DOG uptake by L6 myotubes as these two are important markers for insulin action. In GFP-Glut4 plasmid transfected L6 myotubes, insulin effected Glut4 migration from cytosol to membrane was prevented by palmitate while in cells cotransfected with mutated PKCε vector, where serine 729 was replaced by alanine, palmitate did not inhibit insulin stimulated Glut4 migration (Fig. 9A). This was further evident from [^{3}H]-2DOG uptake study in L6 myotubes (Fig. 9B). These findings demonstrate that FA's damage to insulin sensitivity is mediated through PKCε.

4. **Discussion**

Binding of insulin to IR initiates insulin signaling in classical insulin target cells. Several authors have demonstrated an association between FAs and decreased IR in insulin target tissues and cells. These defects in IR impair insulin signaling that compromises insulin sensitivity and insulin resistance (1-13,15). Such a large number of citations favoring the issue that deficiency of IR is related to insulin signaling defect raises a question about the spare receptor in target cells. Concept of spare receptor in insulin target cells does not hold good any more, insulin occupation of all high affinity receptor binding sites is required to ensure full receptor kinase activation thus void the possibility of spare receptor in skeletal muscle (32,33) and hepatocytes (34). Since one high affinity IR is for one molecule of insulin (35), detection of absence of spare receptor is meaningful. Evidences available with adipocytes suggest that spare receptor phenomenon is due to post receptor event (32,36). The reason for this discussion is to

emphasize the biological relevance of large number of above mentioned reports which demonstrated association of FA with IR reduction and found that this deficiency leads to insulin signaling defects which affects insulin sensitivity (4,10-13,15). We have observed that in obese type 2 diabetic *db/db* mice about 85-90% of IRβ has been degraded in skeletal muscle with almost equal amount of reduction in its gene expression and this has strikingly reduced insulin sensitivity. Hence, FA induced degradation of IR would likely implement insulin resistance, a hall mark of type 2 diabetes.

Loss of insulin sensitivity due to FA induced defects in IR signaling pathway is known for a long time. There are reports on the disruption of every molecules of insulin signaling pathway due to FAs (37-39). However, defects of any of them would adversely affect insulin sensitivity. This makes our understanding a little cloudy although there is no confusion that it is FAs which produces this defect as drug induced decrease of circulatory FAs improves insulin sensitivity (40). About a decade ago Ikeda *et al*, 2001 (13), taking well characterized diabetic animal model i.e., sand rat (*P. obesus*) demonstrated that PKCε overexpression and activation has a link with decreased IR expression and that impaired insulin downstream signaling. In fact, there are several reports on PKCε involvement in insulin resistance and type 2 diabetes (4,14,41) on one hand and loss of insulin sensitivity due to FA induced IR degradation on the other (4,10,11) but a link between them remains unclear. Present investigation has contributed to make this understanding clear. We have shown that target of FAs is PKCε, it begins disruption of insulin signals by phosphorylating PKCε in a PDK1 independent pathway. Saturated fatty acids, palmitate and myristate phosphorylated PKCε, an unsaturated fatty acid, oleate also exhibited this property but it has no inhibitory effect on IR expression.

However, oleate adverse effect on insulin sensitivity could be due to serine/threonine phosphorylation of IRS1 as reported by Ragheb et al, 2009 (42). Once phosphorylated, pPKCε moves to the nuclear region. It was surprising to detect it there as PKCε lacks NLS. We then understand the purpose of FA induced phosphorylation of PKCε and why it is localized in the nuclear region as a complex with F-actin. F-actin which has 13 NLS and it recognizes only phospho-form of PKCε because phosphorylation exposes hexapeptide F-actin binding motif at regulatory domain of PKCε. This permits F-actin binding and transport of pPKCε to the nuclear region (27,29). In the nuclear region, pPKCε plays a key role, it phosphorylates HMGA1 and downregulates its expression by deactivating its transcriotion factor Sp1. Phosphorylation of HMGA1 by PKCs has been amply reported earlier and this restricted its mobility (43,44). Phosphorylated HMGA1 preferentially interacts with positively charged histone that effected increase of its residence time in heterochromatin region (45). Regulation of HMGA1 expression is dependent on the cooperation between Sp1 and AP1 transcription factors (46) and phosphorylation of Sp1 has been shown to inhibit its DNA binding activity (47). These together attenuated IR gene and protein expression which seriously compromised insulin sensitivity. Novelty of our work lies in deciphering the underlying mechanism on FA induced IRβ downregulation, the central regulator is phospho-PKCε which forms connection between them and disrupt insulin signaling by impairing HMGA1. We have demonstrated that through this pathway FA caused insulin resistance in classical target cells.

Acknowledgement

We thank Dr. Partha P. Banerjee (Georgetown University Medical Center, Washington, DC, U.S.A.) for providing L6, HepG2 and 3T3-L1 cell lines, Dr Jeffrey E. Pessin (Albert Einstein College of Medicine, New York, NY, U.S.A.) for the GFP–GLUT4 vector and Prof. Graeme Bell (University of Chicago, Illinois, USA) for the gift of human insulin receptor promoter plasmid construct phINSRP-1. The author, Suman Dasgupta is thankful to University Grants Commission, New Delhi, for the award of Research Fellowships. Samir Bhattacharya gratefully acknowledges the Indian National Science Academy for his INSA Senior Scientist position. This research work was financially supported by the grant from Department of Science and Technology (Grant No. VI-D&P/137/06-07/TDT), Ministry of Science and Technology, Govt. of India and a grant from National Institute of Plant Genome Research, New Delhi. The authors are grateful to Dr. A. Bandyopadhyay, and Dr. S. Roy of Indian Institute of Chemical Biology, Kolkata for their help in the experimental work. The authors appreciate the facilities extended by the Head, Department of Zoology, Visva-Bharati University, Santiniketan; the Director, National Institute of Plant Genome Research, New Delhi, the Director, National Institute of Immunology, New Delhi.

References

[1]. O.G. Kolterman, G.M. Reaven, J.M. Olefsky, Relationship between in vivo insulin resistance and decreased insulin receptors in obese man, J. Clin. Endocrinol. Metab. 48 (1979) 487-494.

[2] Y. Le Marchand-Brustel, T. Grémeaux, R. Ballotti, E. Van Obberghen, Insulin receptor tyrosine kinase is defective in skeletal muscle of insulin-resistant obese mice, Nature 315 (1985) 676-679.

[3] M. Dodson Michael, R.N. Kulkarni, C. Postic, S.F. Previs, G.I. Shulman, M.A. Magnuson, C. R. Kahn, Loss of insulin signaling in hepatocytes leads to severe insulin resistance and progressive hepatic dysfunction, Molecular Cell 6 (2000) 87–97.

[4] D. Dey, M. Mukherjee, D. Basu, M. Datta, S.S. Roy, A. Bandyopadhyay, S. Bhattacharya, Inhibition of insulin receptor gene expression and insulin signaling by fatty acid: interplay of PKC isoforms therein, Cell Physiol. Biochem. 16 (2005) 217-228.

[5] L. Zhou, J. Zhang, Q. Fang, M. Liu, X. Liu, W. Jia, L.Q. Dong, F. Liu, Autophagy-mediated insulin receptor down-regulation contributes to endoplasmic reticulum stress-induced insulin resistance, Mol. Pharmacol. 76 (2009) 596–603.

[6] J.M. Podskalny, C.R. Kahn, Cell culture studies on patients with extreme insulin resistance. I. Receptor defects on cultured fibroblasts, J. Clin. Endocrinol. & Metabolism 54 (1982) 261-268.

[7] K. Ojamaa, J.A. Hedo, C.T. Roberts, V.Y. Moncada, P. Gorden, A. Ullrich, S.I. Taylor, Defects in human insulin receptor gene expression, Mol. Endocrinol. 2 (1988) 242-247.

[8] D. Foti, E. Chiefari, M. Fedele, R. Iuliano, L. Brunetti, F. Paonessa, G. Manfioletti, F. Barbetti, A. Brunetti, C.M. Croce, A. Fusco, A. Brunetti, Lack of architectural factor HMGA1 causes insulin resistance and diabetes in human and mice, Nat. Med. 11 (2005) 765–773.

[9] I. L. Becker, S. Brodesser, D. Lütjohann, M. Azizov, J. Buchmann, E. Hintermann, K. Sandhoff, A. Schürmann, J. Nowock, G. Auburger, Insulin receptor and lipid metabolism pathology in ataxin-2 knock-out mice, Human Molecular Genetics 17 (2008) 1465–1481.

[10] M.W. Ruddock, A. Stein, E. Landaker, J. Park, R.C. Cooksey, D. McClain, M.E. Patti, Saturated fatty acids inhibits hepatic insulin action by modulating insulin receptor expression and post-receptor signaling, J. Biochem. 144 (2008) 599-607.

[11] M.M. Hennes, E. Shrago, A.H. Kissebah, Receptor and postreceptor effects of free fatty acids (FFA) on hepatocyte insulin dynamics, Int. J. Obes. 14 (1990) 831-841.

[12] C. Pramfalk, J. Lanner, M. Andersson, E. Danielsson, C. Kaiser, I.M. Renström, M. Warolén, S.R. James, Insulin receptor activation and down-regulation by cationic lipid transfection reagents, BMC Cell Biology 5 (2004) 1-8.

[13] Y. Ikeda, G.S. Olsen, E. Ziv, L.L. Hansen, A.K. Busch, B.F Hansen, E. Shafrir, S.L. Mostaf, Cellular mechanism of nutritionally induced insulin resistance in *Psammomys Obesus,* Diabetes 50 (2001) 584–592.

[14] V.T. Samuel, Z.X. Liu, A. Wang, S.A. Beddow, J.G. Geisler, M. Kahn, X. Zhang, B.P. Monia, S. Bhanot, G.I. Shulman, Inhibition of protein kinase Cε prevents hepatic insulin resistance in nonalcoholic fatty liver disease, J. Clin. Invest. 117 (2007) 739–745.

[15] D. Dey, A. Bhattacharya, S.S. Roy, S. Bhattacharya, Fatty acid represses insulin receptor gene expression by impairing HMGA1 through protein kinase Cε, Biochem. Biophys. Res. Commun. 357 (2007) 474-479.

[16] J.A. Chavez, T.A. Knotts, L.P. Wang, G. Li, R.T. Dobrowsky, G.L. Florant, S.A. Summers, A role for ceramide, but not diacylglycerol, in the antagonism of insulin signal transduction by saturated fatty acids, J. Biol. Chem. 278 (2003) 10297–10303.

[17] S. Dasgupta, S. Bhattacharya, A. Biswas, S.S. Majumdar, S. Mukhopadhyay, S. Ray, S. Bhattacharya, NF-κB mediates lipid-induced fetuin-A expression in hepatocytes that impairs adipocyte function effecting insulin resistance. Biochem. J. 429 (2010) 451–462.

[18] O.H. Lowry, N.J. Rosebrough, A.E. Farr, R.J. Randall, Protein measurement with Folin phenol reagent. J. Biol. Chem. 193 (1951) 265–275.

[19] P. Barma, S. Bhattacharya, A. Bhattacharya, R. Kundu, S. Dasgupta, A. Biswas, S. Bhattacharya, S.S. Roy, S. Bhattacharya, Lipid induced overexpression of NF-κB in skeletal muscle cells is linked to insulin resistance. Biochim. Biophys. Acta. 1792 (2009) 190–200.

[20] F. Zhou, Y. Xue, X. Yao, Y. Xu, CSS-Palm: Palmitoylation site prediction with a clustering and scoring strategy (CSS). Bioinformatics 22 (2006) 894–896.

[21] G. Bandyopadhyay, T. Biswas, K.C. Roy, S. Mandal, C. Mandal, B. C. Pal, S. Bhattacharya, S. Rakshit, D. K. Bhattacharya, U. Chaudhuri, A. Konar, S. Bandyopadhyay, Chlorogenic acid inhibits Bcr-Abl tyrosine kinase and triggers p38 mitogen-activated protein kinase–dependent apoptosis in chronic myelogenous leukemic cells, Blood 104 (2004) 2514-2522.

[22] J.D. Dignam, R.M. Lebovitz, R.G. Roeder, Accurate transcription initiation by RNA polymerase D in a soluble extract from isolated mammalian nuclei, Nucleic Acids Res. 11 (1983) 475–489.

[23] X. Qiao, X. Wang, Z. Xu, Y. Yang, Resistin does not down-regulate the transcription of insulin receptor promoter, J. Zhejiang. Univ. Sci. B. 9 (2008) 313-318.

[24] S.M. Turpin, G.I. Lancaster, I. Darby, M.A. Febbraio, M.J. Watt, Apoptosis in skeletal muscle myotubes is induced by ceramides and is positively related to insulin resistance, Am. J. Physiol. Endocrinol. Metab. 291(2006) E1341 - E1350.

[25] Y. Wu, P. Song, J. Xu, M. Zhang, M.H. Zou, Activation of protein phosphatase 2A by palmitate inhibits AMP-activated protein kinase, J. Biol. Chem. 282 (2007) 9777-9788.

[26] V. Cenni, H. Doppler, E.D. Sonnemburg, N. Maraldi, A.C. Newton, A. Toker, Regulation of novel protein kinase Cε by phosphorylation, Biochem. J. 363 (2002) 537-545.

[27] R. Prekeris, R.M. Hernandez, M.W. Mayhew, M.K. White, D.M. Terriani, Molecular analysis of the interactions between protein kinase Cε and filamentous actin, J. Biol. Chem. 273 (1998) 26790–26798.

[28] D. Geiges, T. Meyer, B. Marte, M. Vanek, G. Weissgerber, S. Stabel, J. Pfeilschifter, D. Fabbro, A. Huwiler, Activation of protein kinase C subtypes α, γ, δ, ε, ζ, and η by tumor-promoting and nontumor-promoting agents, Biochem. Pharmacol. 53 (1997) 865-875.

[29] T.R Xu, M.G Rumsby, Phorbol ester-induced translocation of PKC epsilon to the nucleus in fibroblasts: identification of nuclear PKC epsilon-associating proteins, FEBS Letters 570 (2004) 20–24.

[30] A. Brunetti, G. Manfioletti, E. Chiefari, I.D. Goldfine, D. Foti, Transcriptional regulation of human insulin receptor gene by the high-mobility group protein HMGI(Y), FASEB J. 15 (2001) 492-500.

[31] D. Foti, R. Iuliano, E. Chiefari, A. Brunetti, A nucleoprotein complex containing Sp1, C/EBPβ and HMGI-Y controls human insulin receptor gene transcription, Mol. Cell. Biol. 23 (2003) 2720–2732.

[32] M. Camps, A. Guma, F. Vinals, X. Testar, M. Palacin, A. Zorzano, Evidence for the lack of spare high-affinity insulin receptors in skeletal muscle, Biochem. J. 285 (1992) 993-999.

[33] A. Gumà, F. Viñals, M. Camps, M. Lizarbe, C. Mora, J. Bertran, X. Testar, M. Palacín and A. Zorzano, Effect of benzyl succinate on insulin receptor function and insulin action in skeletal muscle: Further evidence for a lack of spare high-affinity insulin receptors, Mol. Cell. Endocrinol. 91 (1993) 29-33.

[34] S. Kato, T. Nakamura, A. Ichihara, Regulatory relation between insulin receptor and its functional responses in primary cultured hepatocytes of adult rats, J. Biochem. 92 (1982) 699-708.

[35] D.T. Pang, J.A. Shafer, Evidence that insulin receptor from human placenta has a high affinity for only one molecule of insulin, J. Biol. Chem. 259 (1984) 8589-8596.

[36] H.H. Klein, G.R. Freidenberg, M. Kladde, J.M. Olefsky, Insulin activation of insulin receptor tyrosine kinase in intact rat adipocytes. An in vitro system to measure histone kinase activity of insulin receptors activated in vivo, J. Biol. Chem. 261 (1986) 4691-4697.

[37] L.M. Dickson, C.J. Rhodes, Pancreatic β-cell growth and survival in the onset of type 2 diabetes: a role for protein kinase B in the Akt?, Am. J. Physiol. Endocrinol. Metab. 287 (2004) E192-E198.

[38] M.P. Corcoran, S. Lamon-Fava, R.A. Fielding, Skeletal muscle lipid deposition and insulin resistance: effect of dietary fatty acids and exercise, Am. J. Clin. Nutr. 85 (2007) 662-677.

[39] M. F. White, IRS proteins and the common path to diabetes, Am. J. Physiol. Endocrinol. Metab. 283 (2002) E413-422.

[40] R.N. Bergman, M. Ader, Free fatty acids and pathogenesis of type 2 diabetes mellitus, Trends. Endocrinol. Metab. 11 (2000) 351-356.

[41] E. Mack, E. Ziv, H. Reuveni, R. Kalman, M.Y. Niv, A. Jörns, S. Lenzen, E. Shafrir, Prevention of insulin resistance and beta-cell loss by abrogating PKCepsilon-induced serine phosphorylation of muscle IRS-1 in *Psammomys obesus*, Diabetes Metab. Res. Rev. 24 (2008) 577-84.

[42] R. Ragheb, G.M.L. Shanab, A.M. Medhat, D.M. Seoudi, K. Adeli, I.G. Fantus, Free fatty acid-induced muscle insulin resistance and glucose uptake dysfunction: Evidence for PKC activation and oxidative stress-activated signaling pathways, Biochem Biophys Res Commun. 389 (2009) 211-216.

[43] R. Reeves, L. Beckerbauer, HMGI/Y proteins: flexible regulators of transcription and chromatin structure, Biochim. Biophys. Acta. 1519 (2001)13-29.

[44] D.M. Xiao, J.H. Pak, X. Wang, T. Sato, F.L. Huang, H.C. Chen, K.P. Huang, Phosphorylation of HMG-I by protein kinase C attenuates its binding affinity to the promoter regions of protein kinase Cγ and neurogranin/RC3 genes, J. Neurochem. 74 (2000) 392–399.

[45] M. Harrer, H. Luhrs, M. Bustin, U. Scheer, R. Hock, Dynamic interaction of HMGA1a proteins with chromatin, J. Cell. Sci. 117 (2004) 3459–3471.

[46] I. Cleynen, C. Huysmans, T. Sasazuki, S. Shirasawa, W. Van de Ven, K. Peeters, Transcriptional control of the human high mobility group A1 gene: Basal and oncogenic ras-regulated expression, Cancer Res. 67 (2007) 4620-4629.

[47] S.A. Armstrong, D.A. Barry, R.W. Leggett, C.R. Mueller, Casein kinase II-mediated phosphorylation of the C terminus of Sp1 decreases its DNA binding activity, J. Biol. Chem. 272 (1997) 13489–13495.

Figure Legends

Fig 1. Interrelationship between fatty acids, pPKCε and IR in db/db mice. (A) Serum was collected from *db/db* mice and its control littermate (Con) followed by estimation of glucose level. (B) Skeletal muscle cells isolated from control and db/db mice were incubated *in vitro* with [^{3}H]-2DOG followed by the determination of its uptake in a liquid scintillation counter. (C) Skeletal muscle, liver and fat tissues from these mice were subjected to immunoblot analysis using anti-IRβ antibody (upper panel) or qPCR (lower panel) to determine the IRβ protein and mRNA level, β actin and *gapdh* were used as internal control (D,E) Serum FFA level was measured by acyl-CoA synthase and acyl-CoA oxidase methods where palmitate and myristate were found to be the major FAs in the serum of *db/db* mice in comparison to control (F) Immunoblot analysis of PKCε and pPKCε level in above tissues where β actin represent as loading control. Each experimental data represented the mean value of six individual animals. All data represented are means ± SEM of five individual experiments, *$p<0.01$ vs Con.

Fig 2. Palmitate and myristate are key players in lipid induced IRβ reduction. (A) L6 myotube incubated with different FAs, followed by immunoblot analysis with anti-IRβ antibody. (B) L6 myotube, HepG2 and 3T3-L1 cells were incubated without or with palmitate (P) or myristate (M) followed by immunoblot analysis with anti-pPKCε or anti-IRβ antibodies. (C) Total RNA extracted from these cells was subjected to RT-PCR to determine the IRβ mRNA level, *gapdh* was used as internal control. (D) L6 skeletal muscle cells were incubated with two different fatty acids, palmitate and oleate for 4h. Cells without any treatment served as control. On termination of incubation, cells were lysed and immunoblotted with anti-pPKCε antibody, β-actin served as internal control. (E) Effect of varied doses of palmitate on [^{3}H] 2-deoxyglucose (2-DOG) uptake by L6 myotubes. L6 cells were treated with varied concentration of palmitate (0.25 to 1.0 mM) at different time periods (4 to 16h) in the absence (C) or presence of 100nM of insulin. On termination of incubations cells were lysed, centrifuged and radioactivity of the supernatant was counted in a liquid scintillation counter. (F) Examination of cellular apoptosis as determined by caspase 3 activity in response to varied concentrations of palmitate. *$p<0.05$ vs C. (E) All data are Mean± SEM of three individual experiments.

Fig 3. FAs induced IRβ degradation mediated through pPKCε (A) Analysis of pPKCε, PKCε and IRβ levels in L6 myotubes untransfected (UT) or transfected with PKCε site-mutant ($S^{729}A$) or deletion-mutant (ΔS^{729}) followed by incubation without or with palmitate. (B) Incubation of pCMV-PKCε or PKCε siRNA transfected L6 myotubes with palmitate followed by immunoblotting with indicated antibodies. (C) Incubation of L6 myotubes with insulin in absence or presence of palmitate (P) followed by IRβ, IRS1

and Akt immunoblotting. Figures are representative of one of three independent experiments; β actin was used as loading control.

Fig. 4. PKCε acylation causes kinase independent autophosphorylation. **(A)** L6 myotubes were incubated for indicated time periods with radiolabeled [^{14}C]-palmitate. PKCε was immunoprecipitated and subjected to SDS-PAGE followed by fluorography (FG) or immunoblotting (IB). **(B)** Immunoprecipitated PKCε was incubated for 1h at 30°C with either Tris buffer, or neutral 2 M hydroxylamine (HDX) or 2 N HCl or 2 N NaOH followed by SDS-PAGE and fluorography (FG) or immunoblotting (IB). (**C)** L6 myotubes were incubated without or with palmitate in the absence or presence of cerulenin or triacsin C. On termination of incubations cell lysates were immunoblotted with pPKCε or PKCε antibodies. **(D)** Wild type PKCε vector was mutated at indicated positions to generate mutated forms where cysteine was replaced by alanine through site directed mutagenesis **(E)**. Wild type and mutated vectors transfected L6 myotubes were incubated with [^{14}C]-palmitate. PKCε and pPKCε was immunoprecipitated with respective antibodies followed by SDS-PAGE and fluorography (FG) to detect amount of radiolabeled palmitate incorporation to PKCε (upper panel) or immunoblot (IB) analysis to observe amount of PKCε phosphorylation (lower panel).

Fig. 5. Palmitate induced pPKCε nuclear translocation is mediated through F-actin. **(A)** Nuclear extract isolated from palmitate (P) or myristate (M) incubated L6 myotubes were subjected to immuniprecipitation with anti-F-actin antibody followed by probed with pPKCε or PKCε antibodies. β actin was used as internal control. **(B)** L6 myotubes were

incubated without or with palmitate in the presence or absence of εV1 or Cytochalasin B (CytoB). On termination of incubations cytosolic (Cyt) and nuclear (Nu) fractions were prepared and subjected to immunoblot analysis with pPKCε antibody, β actin was used as internal control. **(C)** L6 myotubes were incubated without (control) or with palmitate, on termination of incubations, cells were fixed and permeabilized. Permeabilized cells were coincubated with anti-rabbit pPKCε and anti-mouse F-actin antibodies for 4h followed by FITC and Rhodamine conjugated respective secondary antibodies for 2h. DAPI was used to stain the nucleus. Figures are representative of one of three independent experiments.

Fig. 6. pPKCε nuclear translocation impairs HMGA1. (A) L6 myotubes incubated with palmitate (P) or myristate (M) without or with εV1. Nuclear fraction was isolated and immunoprecipitated with anti-HMGA1 antibody followed by probing with anti-pPKCε antibody. (B) Pure His-HMGA1 protein was immobilized to the Ni^{2+} coated NTA sensor chip and varied concentrations of pPKCε protein (50, 100, 200, 400nM) was run over it to analyze the binding between them with the help of surface plasmon resonance study. The interactions was monitored in real time via the changes in refractive index which was proportional to the changes in mass concentration at the sensor chip surface and plotted as RU (Resonance unit) versus time. Binding affinity between HMGA1 and pPKCε was determined from the level of binding at equilibrium as a function of sample concentration and referred as equilibrium dissociation constant (K_D) as depicted in the inset. (C) Analysis of HMGA1 protein and mRNA level in L6 myotubes incubated with palmitate in the presence of εV1 or Cerulenin or Triacsin C by immunoblot (upper panel) or RT-PCR (lower panel). (D) L6 myotubes were incubated with palmitate in the presence of

[γ32p]-ATP. On termination of incubation, palmitate induced ^{32}pPKCε was purified from these cells through immunoaffinity chromatography using anti-pPKCε antibody coupled CNBr activated sepharose 4B column. ^{32}pPKCε was incubated with HMGA1 protein for 30 min at 37°C in cell free condition, HMGA1 was pulled down with anti-HMGA1 antibody followed by SDS-PAGE and autoradiographed. PVDF membrane corresponding to the radioactive spots was cut and radiolabeled phosphate incorporated into HMGA1 was measured in a liquid scintillation counter. Data were means ± SEM of three individual observations, *p<0.001; vs HMGA1.

Fig. 7. Reduction of HMGA1 gene expression by pPKCε. (A) Immunoblot analysis of phosphorylated Sp1, Jun and Fos level in L6 myotubes incubated without or with palmitate (P) in absence or presence of εV1. (B) Radiolabeled ^{32}pPKCε prepared according to the above description was incubated for 30 min at 30°C with Sp1 followed by subjected to autoradiography. PVDF membrane corresponding to the radioactive spot was cut and incorporation of radiolabeled phosphate to Sp1 was measured in a liquid scintillation counter. Data represents means ± SEM of three individual experiments, *p < 0.01 vs Sp1**.** (C) Nuclear extracts isolated from control, palmitate or palmitate plus εV1 incubated L6 myotubes were subjected to electrophoretic mobility shift assay (EMSA). Probing with anti-Sp1 antibody showed a shift of the band which indicates specific binding of Sp1 on the HMGA1 promoter.

Fig. 8. pPKCε induced defects on HMGA1 attenuates IRβ promoter activity. (A) L6 myotubes were incubated without or with palmitate in the presence of cerulenin or

triacsin C or CytoB or εV1. On termination of the incubations, chromatin immunoprecipitation assay (ChIP) was performed with cell lysate by immunoprecipitating HMGA1 bound IR promoter region using anti-HMGA1 antibody. The recovered DNA was used as a template for PCR analysis with primers of IRβ promoter. (B) IR promoter (pIRP-GLuc) driven luciferase-expressing plasmid was transfected into L6 myotubes followed by the same regime of incubation as indicated above. On termination of incubation, luciferase activity was measured in a luminometer. Data represents means ± SEM of five individual experiments, *$p < 0.001$ vs C, #$p < 0.01$ vs P.

Fig. 9. Palmitate induced insulin signaling defects was prevented by kinase dead PKCε. (A) GFP-Glut4 vector transfected L6 myotubes were cotransfected with wild or PKCε mutant vector (PKCε-S^{729}A) followed by incubation with insulin (Ins) in the absence or presence of palmitate (P). GFP-Glut4 localization was detected by using Leica laser scanning confocal microscope. (D) Cells from the same incubations with presence of [^{3}H]-2DOG were lysed and counted in a liquid scintillation counter according to the procedure described in the materials and method section. Data represents means ± SEM of five individual experiments, *$p < 0.001$ vs C, #$p < 0.01$ vs Ins.

Fig. 1.

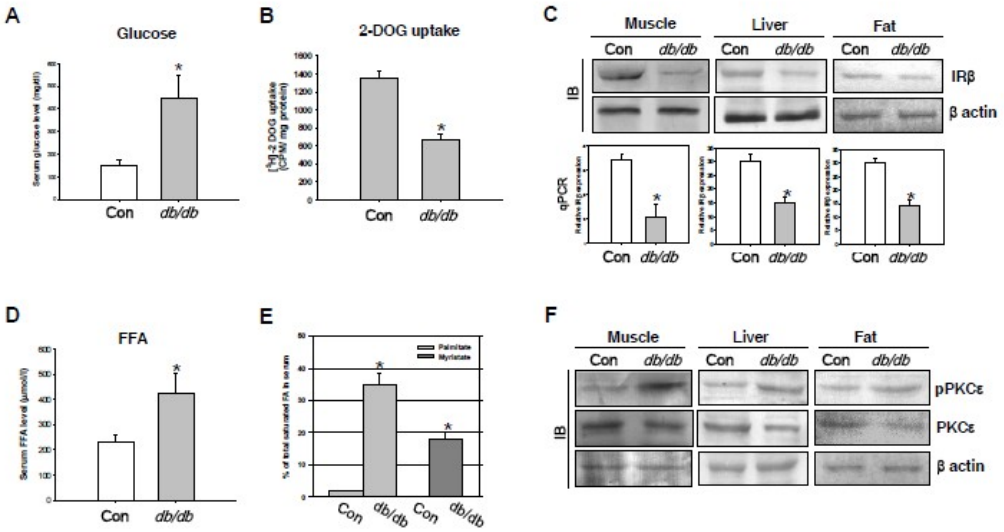

Fig. 2.

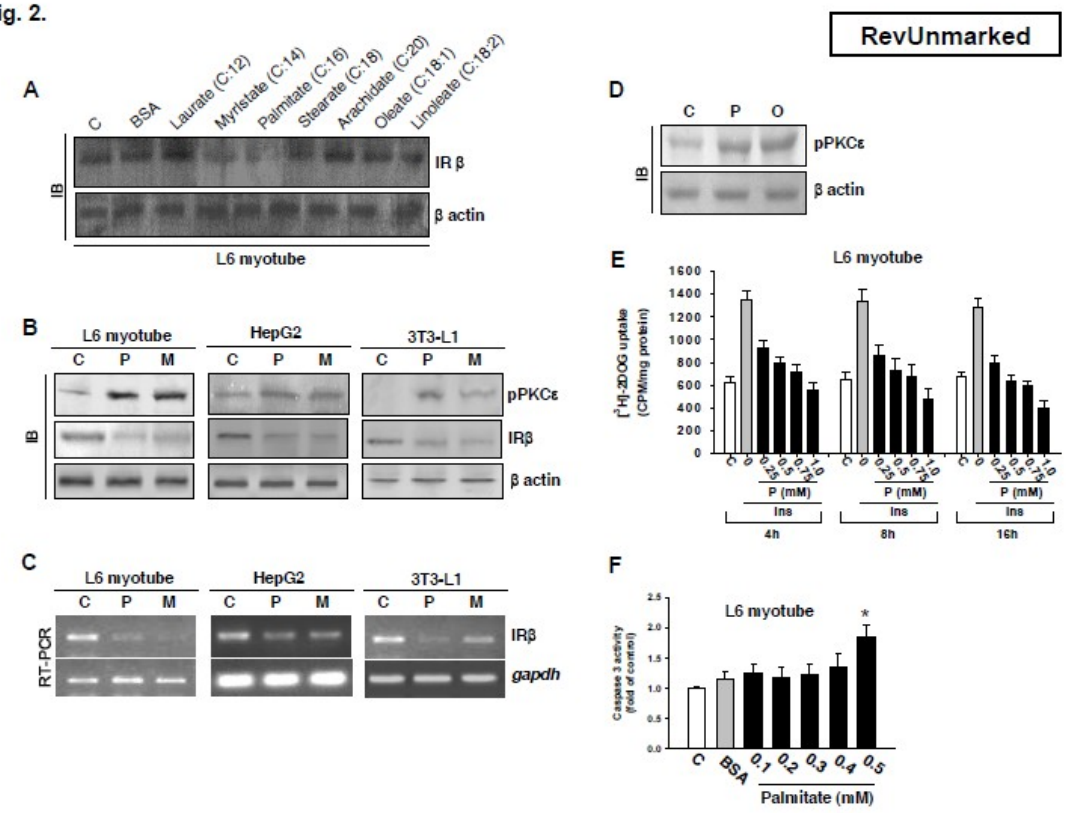

Fig. 3.

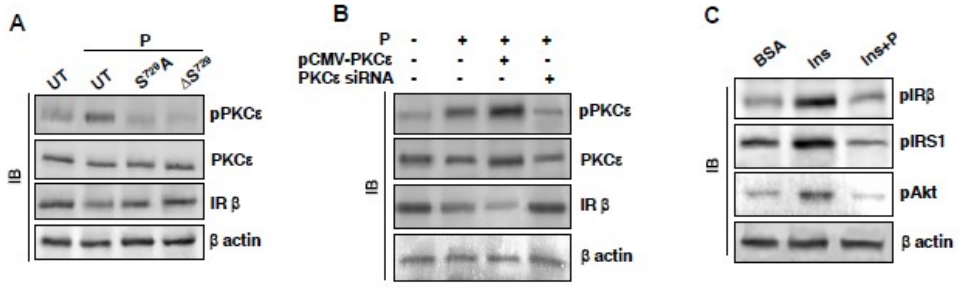

Fig. 4.

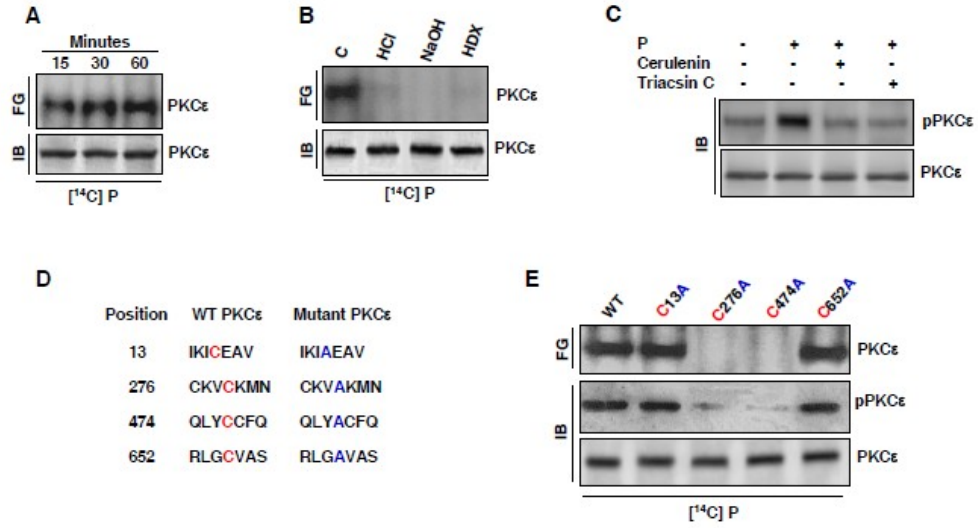

Fig. 5.

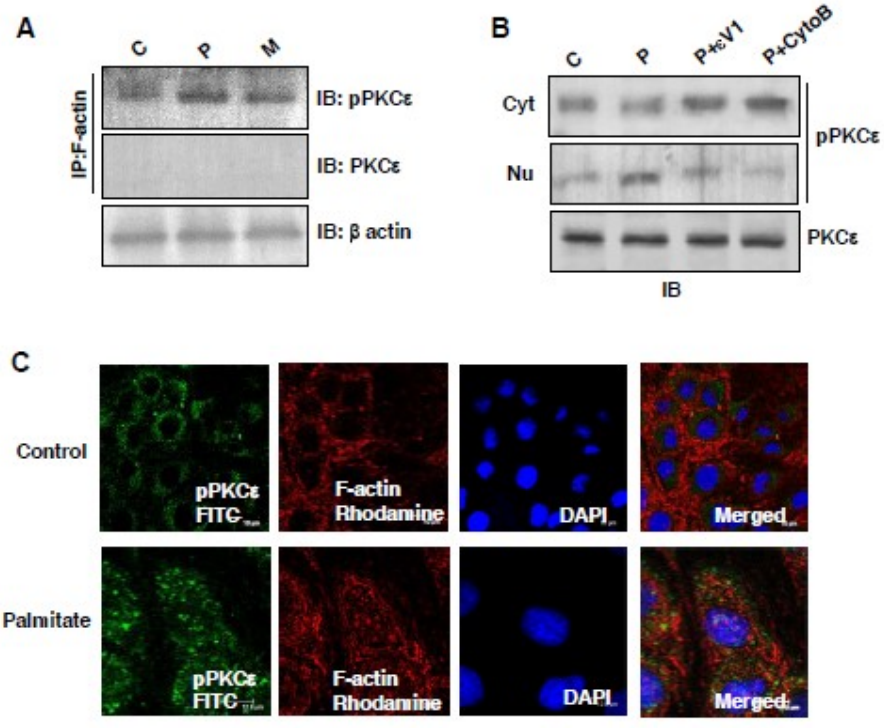

Fig. 6.

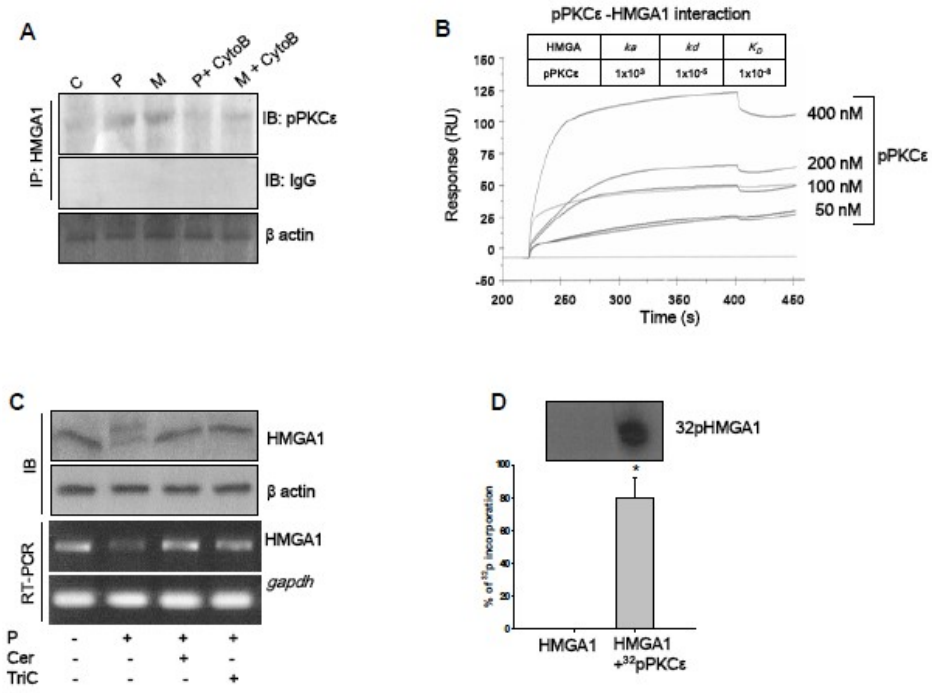

Fig. 7.

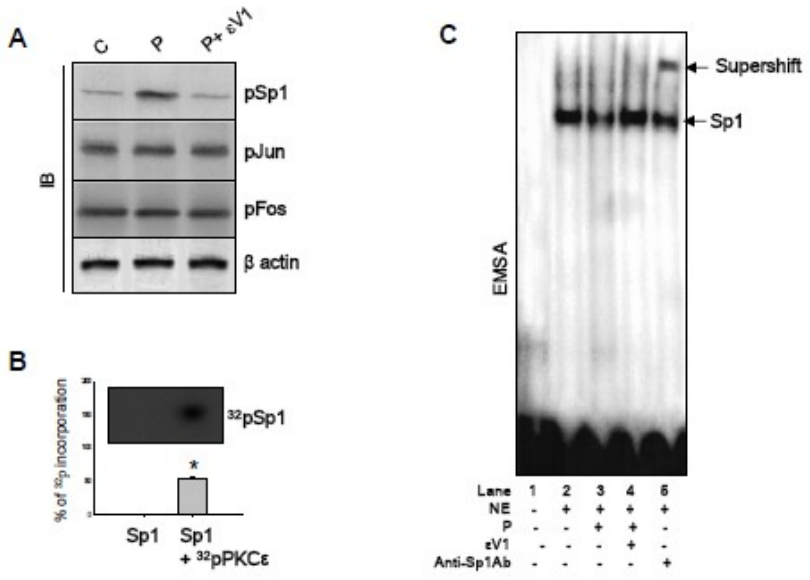

Fig. 8.

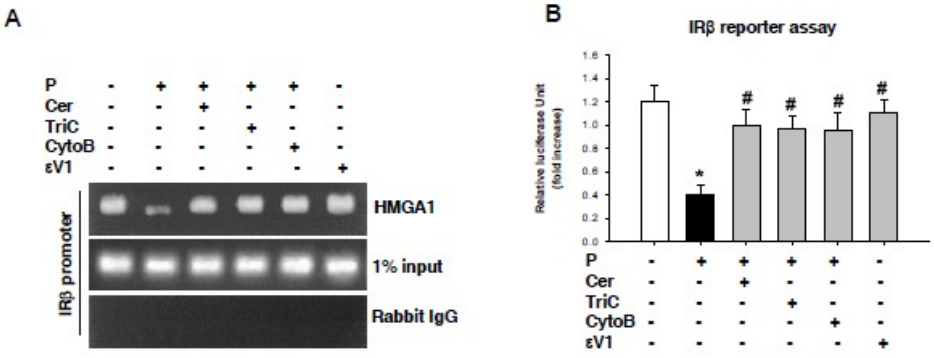

Fig. 9.

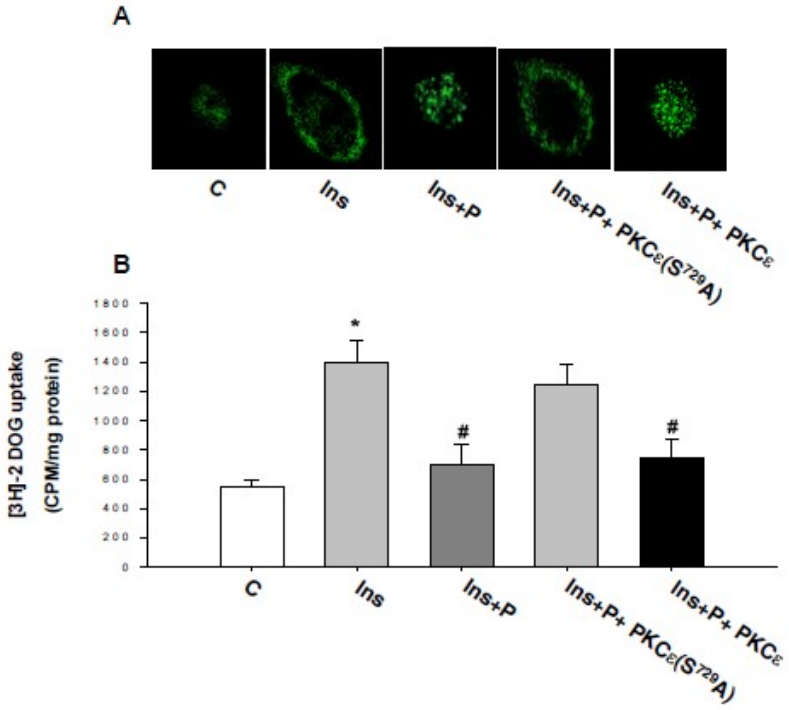

Table 1: Primers used in the present study.

Organism	Primer	Direction	Sequence
Mice	HMGA1	Forward	5'-CCGGCCCCATCTCACTCTGA-3'
		Reverse	5'-GTGTGGGGTAGGTAACCAGT-3'
Rat	HMGA1	Forward	5'-CAGGAAAAGGATGGGACTGA-3'
		Reverse	5'-CAGAGGACTCCTGGGAGATG-3'
Mice	IRβ	Forward	5'-AATGGCAACATCACACACTACC-3'
		Reverse	5'-CAGCCCTTTGAGACA-ATAATCC-3'
Rat	IRβ	Forward	5'-GGATGGTCAGTGTGTGGAGA-3'
		Reverse	5'-TCGTGAGGTTGTGCTTGTTC-3'
Mice	GAPDH	Forward	5'-CCACCCATGGCAAATTCCATGGCA-3'
		Reverse	5'-TCTAGACGGCAGGTCAGGTCCACC-3'
Rat	GAPDH	Forward	5′- GCCATCAACGACCCCTTC-3′;
		Reverse	5′-AGCCCCAGCCTTCTCCA- 3′

Research Highlights:

It is known for a long time that lipid causes insulin resistance and type 2 diabetes. It was indicated that defects in insulin signal is responsible for impairing insulin sensitivity. However, the underlying mechanism of lipid action is yet unclear. In this report we have described the molecular mechanism of lipid induced insulin resistance. We have demonstrated that fatty acid downregulated insulin receptor gene expression through the impairment of HMGA1, the transcriptional regulator of insulin receptor gene. However, key player is the phosphorylated PKCε, fatty acid phosphorylated PKCε through palmitoylation which in turn impaired HMGA1. Fatty acid induced degradation of insulin receptor could not be observed by mutating PKCe phosphorylation site or silencing of PKCe gene expression. The detail of these work and the rationale for the finding have been described in the text.